



# STUDIES ON THE ROLE OF A PHOTON COLLIMATOR FOR THE ILC POSITRON SOURCE

L. Zang\*, I. Bailey, A. Wolski, Cockcroft Institute and University of Liverpool, UK

July 7, 2008

## Abstract

A positron source based on a helical undulator provides the capability of producing a beam of polarised positrons. The degree of polarisation of the positrons depends upon the polarisation of the photons produced from the undulator; the polarisation of the photons in turn depends on the photon energy and production angle. We calculate the photon energy spectrum and polarisation for one design of the helical undulator for the International Linear Collider (ILC), investigate approximations commonly made in calculating these quantities, and explore the role of a photon collimator in improving the positron polarisation.

---

\*l.zang@cockcroft.ac.uk

# 1 Introduction

Production of polarised positrons in the ILC will be achieved by means of a source based on a helical undulator [1]. An electron beam at 150 GeV passing through the undulator will produce a beam of polarised photons; these photons strike a target to produce polarised positrons [2]. A collimator between the undulator and the target can be used to remove the halo of the photon beam. Since the polarisation of photons in the beam is dependent on the angle of the photons with respect to the undulator axis, the collimator may also, in principle, be used to control the polarisation. Collimation at a smaller angle will improve the polarisation of the beam; however, it will also result in a loss of intensity. Optimisation of the positron source will involve finding a balance between polarisation and intensity, and it is therefore necessary to model in detail the photon beam from the undulator, and the effects of the photon collimator. In this paper, we present the energy spectrum, angular distribution, and polarisation of the radiation produced by the helical undulator in the ILC positron source. We compare the results of analytical calculations of these quantities for a finite number of undulator periods, with the results for the limiting case of an undulator with an infinite number of periods. Finally, we discuss the effects of the photon collimator on the polarisation and intensity of the beam, comparing analytical results with the results of simulations using Fluka. The energy distribution, angular distribution and polarisation of photons from a helical undulator can be derived from the functions  $A_x$  and  $A_y$ , given by [3, 4]:

$$A_x(\omega, \theta; n) = \frac{e}{\pi\sqrt{c}} \left( \frac{\gamma}{K} \eta \theta - n \right) J_n(\eta \theta) [\text{sin}], \quad (1)$$

$$A_y(\omega, \theta; n) = -i \frac{e}{\pi\sqrt{c}} \eta J'_n(\eta \theta) [\text{sin}], \quad (2)$$

where  $J_n(x)$  is a Bessel function,

$$[\text{sin}] = \frac{\sin [N\pi (\zeta - n)]}{(\zeta - n)}, \quad (3)$$

and  $K$  is the undulator parameter,  $N$  is the number of periods in the undulator,  $\gamma$  is the relativistic factor of the electron beam,  $\omega$  is the frequency of the radiation,  $\theta$  is the angle of the radiation to the undulator axis, and  $n$  is a positive integer, identified with harmonics in the radiation. The parameters  $\zeta$  and  $\eta$  are given by:

$$\zeta = (1 - \beta^* \cos \theta) \frac{\omega}{\omega_0} \approx \frac{(1 + K^2 + \gamma^2 \theta^2)}{2\gamma^2} \frac{\omega}{\omega_0}, \quad (4)$$

$$\eta = \frac{K}{\gamma} \frac{\omega}{\omega_0}, \quad (5)$$

where  $\omega_0$  is the angular frequency of the helical orbit of an electron in the undulator:

$$\omega_0 = \frac{2\pi\beta^*c}{\lambda_u}. \quad (6)$$

$\lambda_u$  is the undulator period, and  $\beta^*$  is related to the normalised velocity  $\beta = v/c$  of the electron:

$$\beta^* = \beta \sqrt{1 - \left(\frac{K}{\gamma}\right)^2}. \quad (7)$$

The intensity as a function of photon energy and angle is given by:

$$\frac{dI(\omega)}{d\Omega} = \sum_{n=1}^{\infty} |A_x|^2 + |A_y|^2. \quad (8)$$

Eq. (8) can be integrated over all positive frequencies to get the angular distribution of radiated power; integrated over all angles to produce the power spectrum as a function of frequency; or integrated over all frequencies and angles to find the total radiation intensity. The presence of the sin function [sin] expresses the fact that the energy of the radiation is correlated with the angle. This correlation becomes stronger with increasing number of periods in the undulator, since for large  $N$ , the function [sin] becomes large at frequencies for which  $\zeta \approx n$ , i.e.:

$$\omega \approx \frac{2\gamma^2}{1 + K^2 + \gamma^2\theta^2} \cdot n\omega_0. \quad (9)$$

For given  $K$  and  $\gamma$ , the dominant frequencies in the radiation spectrum are integer multiples of a fundamental frequency that is a function of  $\theta$ . For  $K \approx 1$  (which is the case for the ILC positron source),  $\theta \ll 1/\gamma^2$  and large  $N$ , we have  $\omega \approx \gamma^2 n\omega_0$ . Note that  $\omega$  falls with increasing  $\theta$ .

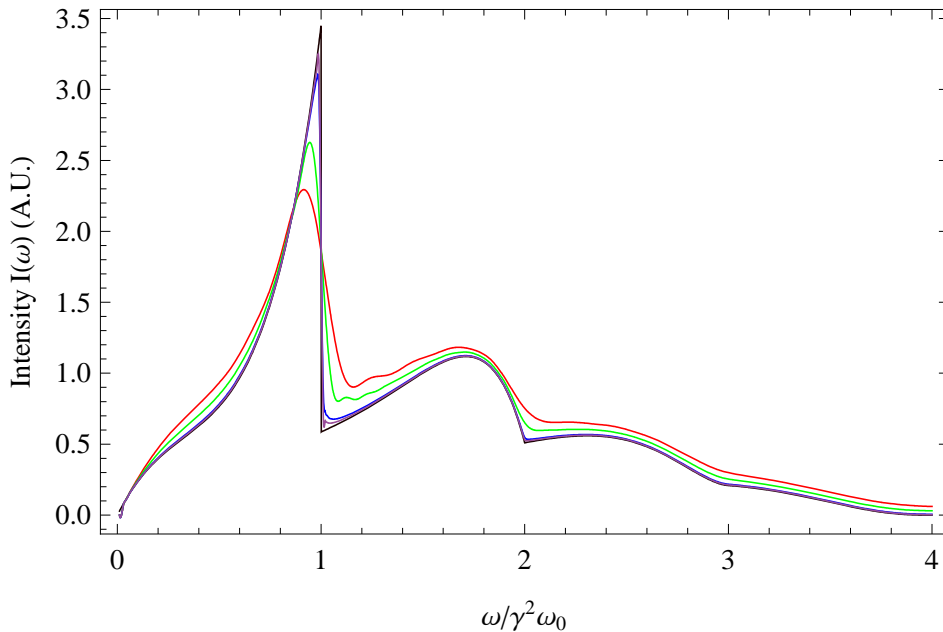


Figure 1: Intensity spectrum of helical undulator radiation.

Figure 1 shows the intensity spectrum (up to the fourth harmonic, and normalised to the number of periods) for helical undulators with  $K = 1$ , and  $N = 5, 10, 50$  and  $100$ . The shape of the spectrum already approaches the large  $N$  limit for  $N = 100$ . For the ILC, where each section of undulator has 200 periods, the large  $N$  limit can be used without significant loss of accuracy: at the first harmonic peak, for example, the large  $N$  approximation differs from a more exact calculation for  $N = 100$  by 4.3%. The large  $N$  approximation is helpful, since taking the limit  $N \rightarrow \infty$  simplifies some of the formulae, and greatly accelerate the calculations.

Figure 2 shows the intensity of each harmonic in the undulator radiation as a function of angle  $\theta$  with respect to the undulator axis.

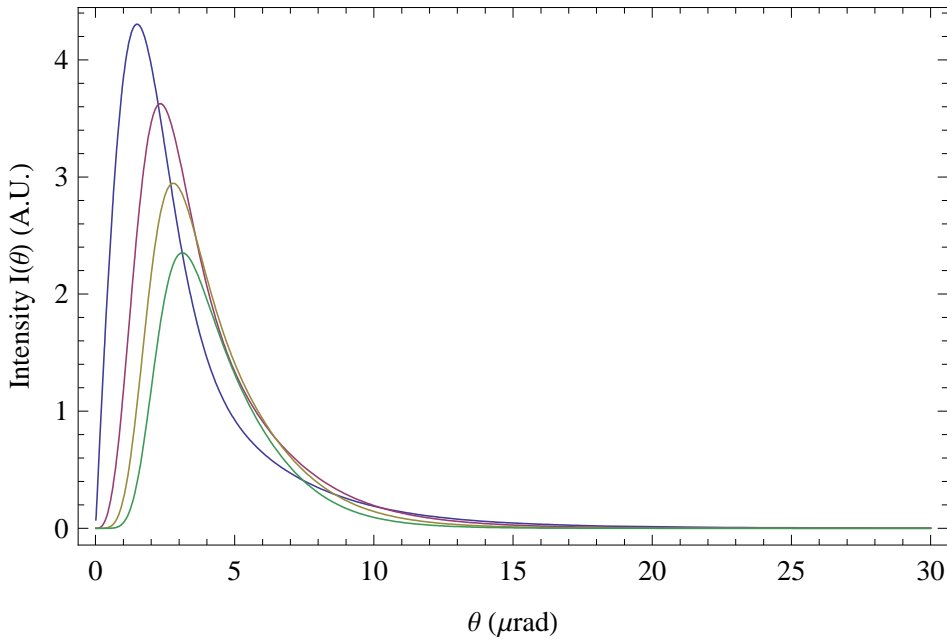


Figure 2: Radiation intensity as a function of  $\theta$ . 1<sup>st</sup>, 2<sup>nd</sup>, 3<sup>rd</sup> and 4<sup>th</sup> harmonics are shown in blue, red, yellow and green respectively.

The circular polarisation of the photon beam, as a function of energy and angle, is given by:

$$P_3 = i \frac{\sum_{n=1}^{\infty} (A_x^* A_y - A_x A_y^*)}{\sum_{n=1}^{\infty} |A_x|^2 + |A_y|^2} \quad (10)$$

We can integrate Eq. (10) over angle, to find the polarisation as a function of frequency; and integrate over frequency to find the polarisation as a function of angle. The results, for the ILC undulator, are shown in Figures 3 and 4 respectively. Again, for the ILC, we use the large  $N$  limit: making the large  $N$  approximation gives a results for the polarisation that differs by 0.015 from the result of a calculation using the more exact formula with  $N = 100$ .

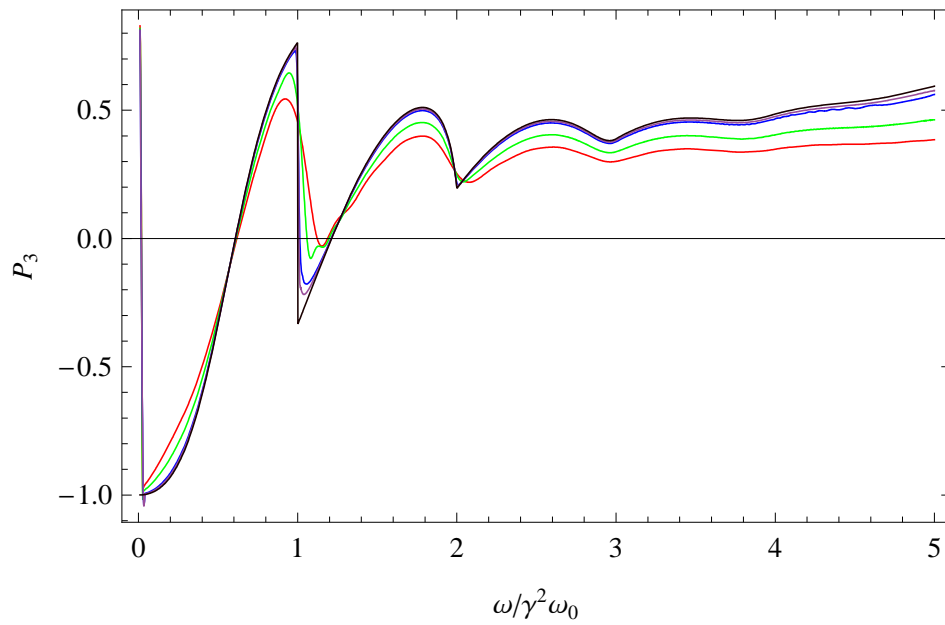


Figure 3: Polarisation as a function of normalised frequency. Different colours show different numbers of periods,  $N = 5$  (red), 10 (green), 50 (blue), 100 (purple),  $\infty$  (black).

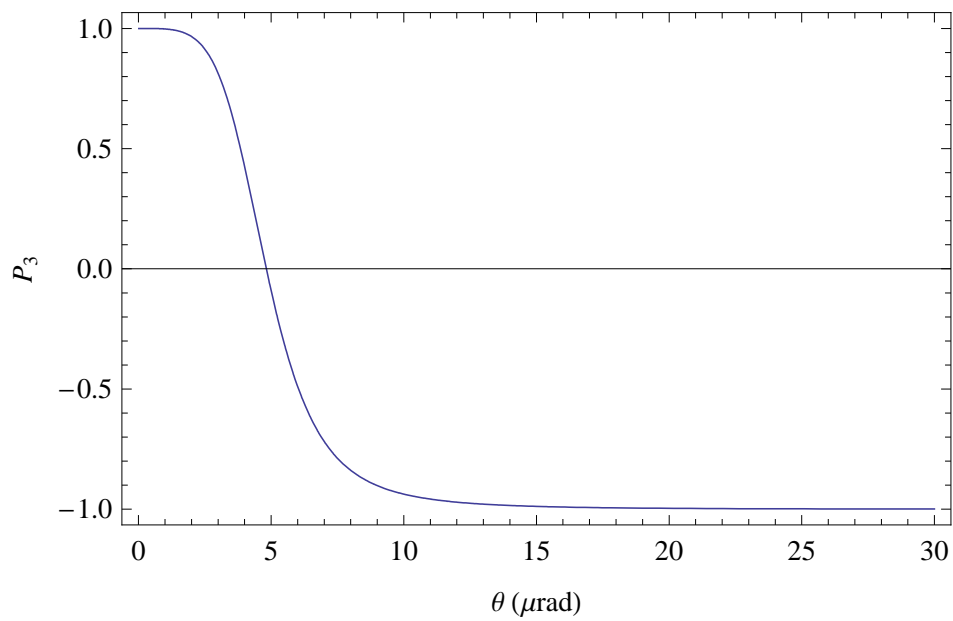


Figure 4: Circular polarisation as a function of angle  $\theta$ .

## 2 Photon Collimation Effects

A photon collimator can affect the intensity and polarisation, since these quantities are functions of angle. Design issues for a photon collimator include collimation efficiency and energy deposition. One proposed design for the ILC positron source is shown in Figure 5. This design consists of a set of spoilers surrounded by an absorber of length 90 cm, inner radius 2 cm and outer radius 6 cm [6]. Copper is used for the absorber, since it has high thermal conductivity (400 W/m/K) and high melting point (1360 K). The spoiler material needs high  $Z$ , good thermal conductivity, and high melting point; titanium is suitable in this case. The spoilers are cylinders of length 1 cm, separated by gaps of 6 cm. The aperture of the spoilers is fixed to optimise the properties of the photon beam.

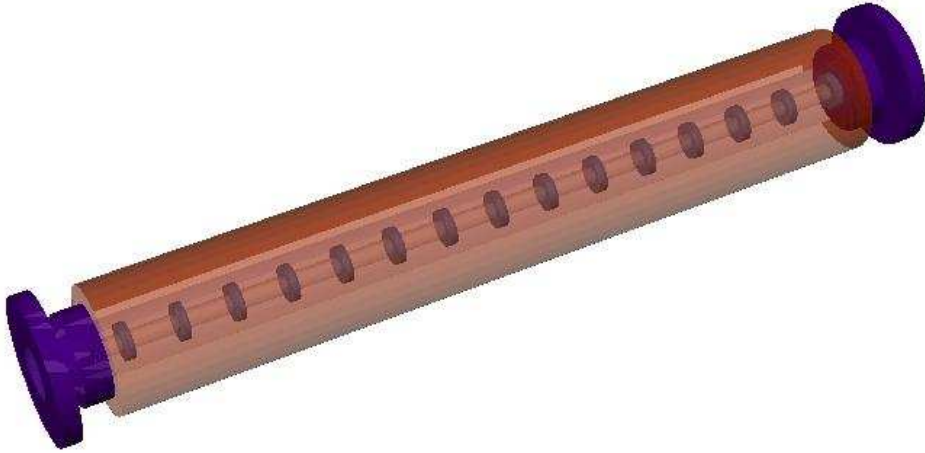


Figure 5: ILC photon collimator.

The variation of transmitted intensity and polarisation with spoiler aperture are shown in Figure 6. Note that this figure shows the results of an analytical calculation using the above formulae, together with the results of a simulation using Fluka [7]; the analytical results and the simulation results are in good agreement.

The choice of aperture depends on the relative weight given to the polarisation and the intensity. Although a high polarisation can be achieved by collimating to very small angles, the drop in photon intensity could make it difficult to meet the specifications for positron intensity. More detailed studies are required to determine the optimum balance between intensity and polarisation (which will depend on the physics studies to be performed); but as an example, if we assume a roughly equal weight given to the polarisation and the intensity, the optimum aperture for the collimator is around 2.35 mm [5]. This corresponds to a maximum angle  $\theta_{max}$  for the photon beam, such that  $\gamma\theta_{max} \approx 1.41$ . In this case, the intensity and polarisation of the transmitted photon beam, as functions of photon frequency, are shown in Figures 7 and 8 respectively.

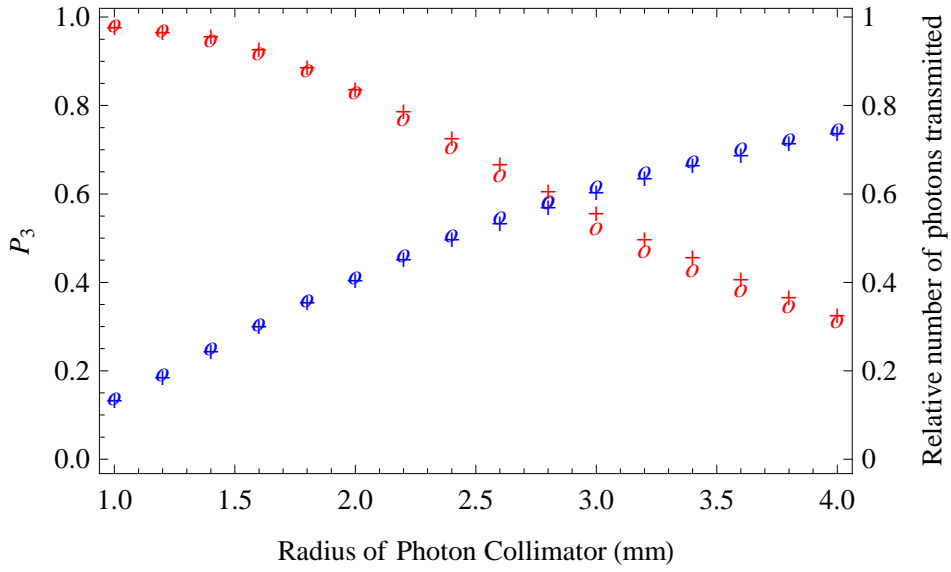


Figure 6: Polarisation (red) and number of photons transmitted (blue) as a function of collimator aperture. The number of photons transmitted is normalised to the uncollimated beam. Analytical results (circles) are compared with Fluka simulation (crosses).

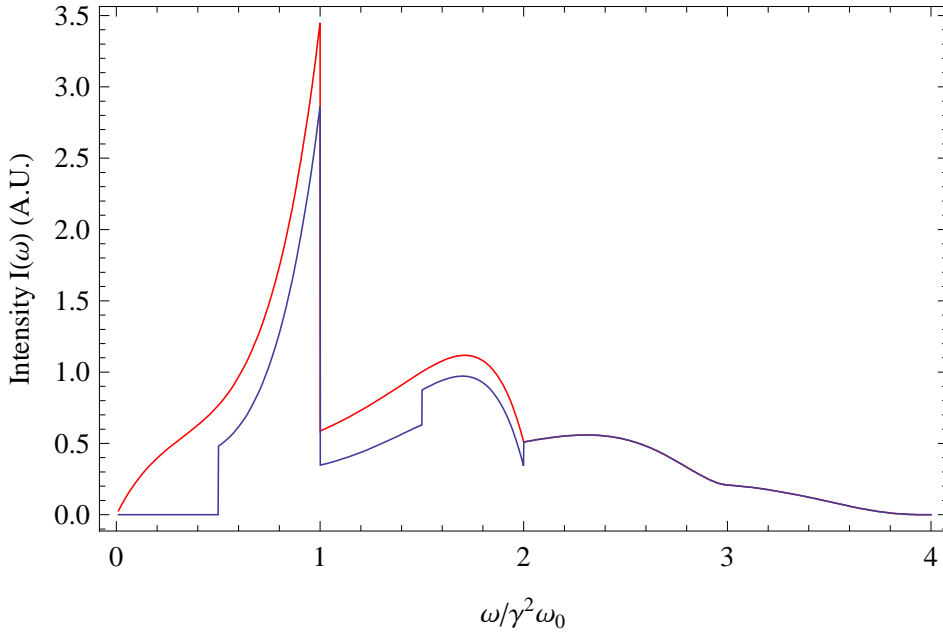


Figure 7: Intensity of radiation from the ILC helical undulator, as a function of normalised frequency. Red: uncollimated. Blue: collimated such that  $\gamma\theta \leq 1.41$ .

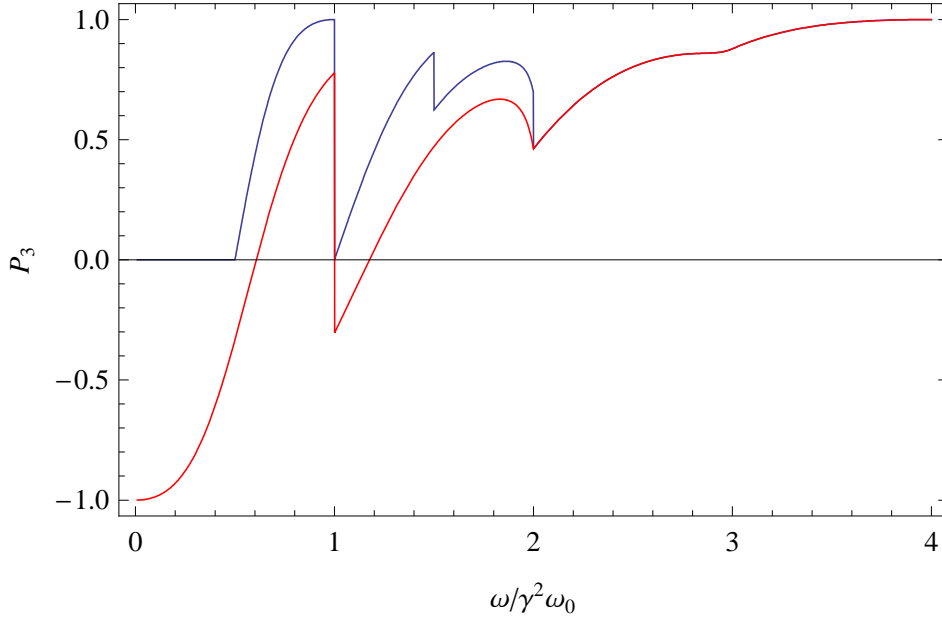


Figure 8: Polarisation of radiation from the ILC helical undulator, as a function of normalised frequency. Red: uncollimated. Blue: collimated such that  $\gamma\theta \leq 1.41$ .

### 3 Conclusion

The formulae for intensity and polarisation of radiation from a helical undulator are well-established. In the case of the ILC polarised positron source, the undulator is in sections of roughly  $N = 200$  periods; we find that the spectra of the radiation and the polarisation can be calculated, to a good approximation, by taking the limit  $N \rightarrow \infty$ . This allows analytical calculations of the effects of photon collimation to be performed very efficiently.

The analytical calculations show good agreement with simulations, using Fluka, based on a proposed design for the photon collimator. Our results show how the polarisation and the intensity of the transmitted photon beam depend on the aperture of the collimator. A high degree of polarisation is possible in principle, but at the cost of a significant drop in intensity.

Other issues associated with the collimator include energy deposition, and production of showers of secondary particles. These effects remain to be studied in detail, before an optimised design for the ILC photon collimator can be achieved.

### Acknowledgement

This work is supported by the Commission of the European Communities under the 6<sup>th</sup> Framework Programme "Structuring the European Research Area", contract number RIDS-011899.

## References

- [1] ILC Reference Design Report (2008).  
<http://www.linearcollider.org/cms/?pid=1000025>
- [2] A. Ushakov, et al., “Polarized Positron Production and Tracking at the ILC Positron Source”, in Proceedings of PAC 07, Albuquerque, New Mexico, USA, 2007.
- [3] B. M. Kincaid, “A short-period helical wiggler as an improved source of synchrotron radiation”, J. App. Phys. 48, 7, 2684, 1977.
- [4] R. P. Walker, “Insertion devices: undulators and wigglers”, in Proceedings of the CERN Accelerator School: Synchrotron radiation and free electron lasers, Grenoble, France, 1996, CERN 98-04.
- [5] J. C. Sheppard, “Helical undulator radiation”, Linear Collider Collaboration Tech Note, LCC-0095, July 2002.
- [6] N. Golubeva and V. Balandin (DESY), private correspondence, 2007.
- [7] A. Ferrari, Paola R. Sala, A. Fasso, J. Ranft, “FLUKA: a multi-particle transport code”, CERN-2005-010, INFN TC\_05/11, SLAC-R-773, 12 October 2005.